International Journal of Pharmaceutics 370 (2009) 93–102

Contents lists available at ScienceDirect

International Journal of Pharmaceutics

journal homepage: www.elsevier.com/locate/ijpharm

Inhibiting efflux with novel non-ionic surfactants: Rational design based on vitamin E TPGS

Michael F. Wempe[a,b,*], Charles Wright[a], James L. Little[a], Janet W. Lightner[b], Shannon E. Large[a], George B. Caflisch[a], Charles M. Buchanan[a], Peter J. Rice[b,e], Vincent J. Wacher[c], Karen M. Ruble[a], Kevin J. Edgar[d]

[a] *Eastman Chemical Company, Kingsport, TN, USA*
[b] *Department of Pharmacology, East Tennessee State University, Johnson City, TN, USA*
[c] *1042 N. El Camino Real, Suite B-174, Encinitas, CA 92024-1322, USA*
[d] *Virginia Tech, 230 Cheatham Hall, Blacksburg, VA 24061, USA*
[e] *School of Pharmacy, University of Colorado Denver, Aurora, CO, USA*

ARTICLE INFO

Article history:
Received 6 October 2008
Received in revised form
14 November 2008
Accepted 18 November 2008
Available online 30 November 2008

Keywords:
P-glycoprotein
Vitamin E TPGS
Efflux ratio
Caco-2 cell monolayers
Liquid chromatography–mass spectrometry/mass spectrometry

ABSTRACT

Tocopheryl Polyethylene Glycol Succinate 1000 (TPGS 1000) can inhibit P-glycoprotein (P-gp); TPGS 1000 was not originally designed to inhibit an efflux pump. Recent work from our laboratories demonstrated that TPGS activity has a rational PEG chain length dependency. In other recent work, inhibition mechanism was investigated and appears to be specific to the ATPase providing P-gp energy. Based on these observations, we commenced rational surface-active design. The current work summarizes new materials tested in a validated Caco-2 cell monolayer model; rhodamine 123 (10 μM) was used as the P-gp substrate. These results demonstrate that one may logically construct non-ionic surfactants with enhanced propensity to inhibit *in vitro* efflux. One new surfactant based inhibitor, Tocopheryl Polypropylene Glycol Succinate 1000 (TPPG 1000), approached cyclosporine (CsA) in its *in vitro* efflux inhibitory potency. Subsequently, TPPG 1000 was tested for its ability to enhance the bioavailability of raloxifene – an established P-gp substrate – *in* fasted male rats. Animals dosed with raloxifene and TPPG 1000 experienced an increase in raloxifene oral bioavailability versus a control group which received no inhibitor. These preliminary results demonstrate that one may prepare TPGS analogs that possess enhanced inhibitory potency *in vitro* and *in vivo*.

1. Introduction

Non-ionic surface-active agents are commonly used in oral formulations to enhance the bioavailability of water insoluble pharmaceutical actives. Non-ionic surfactants offer several advantages: (i) they are more hydrophobic than ionic surfactants; (ii) they possess a better capacity to dissolve water insoluble drugs; and (iii) in general, they are less toxic to biological membranes. Furthermore, by modulating efflux pumps such as P-glycoprotein (P-gp) and/or multi-drug resistance associated proteins (MRP 1 and 2), several non-ionic surfactants (*e.g.* Tweens®, Spans®, Cremophors® (EL and RH40), Pluronic® block copolymers, and vitamin E TPGS) have been shown to influence drug pharmacokinetics (PK) (Miller et al., 1999; Rege et al., 2002; Bogman et al., 2003).

Intestinal P-gp, an ATP-binding cassette (ABC) superfamily (Higgins, 1992) member, has very broad substrate specificity and located at the enterocyte apical membrane. P-gp, the product of the multi-drug resistance gene (MDR1), has been extensively studied (Ueda et al., 1986). P-gp has been found in numerous epithelia including the small intestine luminal surface, colon, brain capillary endothelial cells, and kidney proximal tubules (Thiebaut et al., 1987; Van der Valk et al., 1990; Lankas et al., 1998; Choo et al., 2000; Campbell et al., 2003; Mizuno et al., 2003; Fromm, 2004). P-gp protects cells against toxins by actively transporting against a concentration gradient (Roninson, 1987). By the same mechanism,

Abbreviations: TPGS, tocopheryl polyethylene glycol succinate; Rho, rhodamine 123; ABC, ATP-binding cassette; P-gp, P-glycoprotein; MDR1, multi-drug resistance gene; SAR, structure–activity relationship; Caco-2, human colon adenocarcinoma cell line; ER, efflux ratio; P_{app}, apparent permeability; DCC, *N,N′*-dicyclohexylcarbodiimide; DMAP, 4-dimethylaminopyridine; HEPES, *N*-2-hydroxyethylpiperazine-*N′*-2-ethane sulfonic acid; DMEM, Dulbecco's modified eagle medium; FBS, heat-inactivated fetal calf serum; PET, polyethylene terephthalate; TEER, transepithelial electrical resistance; LC/MS/MS, liquid chromatography–mass spectrometry/mass spectrometry; ESI, electrospray ionization; NMR, nuclear magnetic resonance; CsA, cyclosporine A; CMCe, carboxymethyl cellulose; MCC, microcrystalline cellulose; HBenBCD, hydroxybutenyl-*beta*-cyclodextrin; CMC, critical micelle concentration.

* Corresponding author at: Eastman Chemical Company, Research Laboratories, P.O. Box 1972, Kingsport, TN 37662, USA. Tel.: +1 423 224 7297; fax: +1 423 229 4558.
E-mail addresses: mwempe@eastman.com, wempe@etsu.edu (M.F. Wempe).

0378-5173/$ – see front matter © 2008 Elsevier B.V. All rights reserved.
doi:10.1016/j.ijpharm.2008.11.021

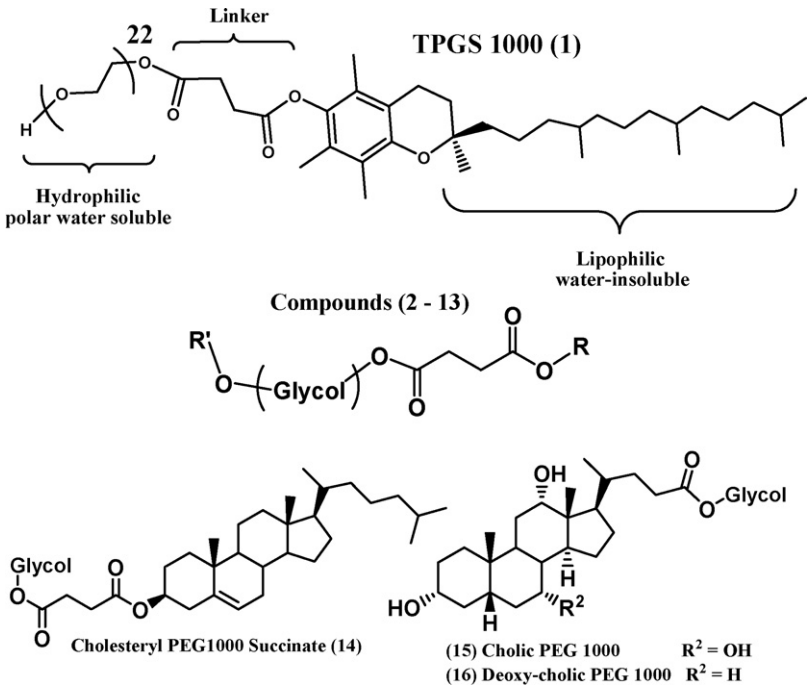

Fig. 1. Surface-active excipients.

P-gp can limit drug oral absorption (Suzuki and Sugiyama, 2000). Therefore, intestinal P-gp inhibition to enhance drug bioavailability has been an attractive therapeutic strategy.

Water soluble TPGS 1000 (D-α-tocopheryl polyethylene glycol 1000 succinate; Fig. 1, (**1**)) has a hydrophilic (PEG) head and a lipophilic (phytyl) tail. TPGS has been used as a solubilizer, an emulsifier, and as a vehicle in lipid based drug delivery formulations. Recently, it was discovered that TPGS inhibits P-gp with modest potency. TPGS, a solubilizer with an excellent safety profile, has been used clinically to enhance the bioavailability of amprenavir, a marketed antiviral drug (Yu et al., 1999; Brouwers et al., 2006). Presumably due in part to limited TPGS potency, amprenavir capsules are large and the common adult dose has been eight capsules, twice a day.

We have previously reported initial work on the structure–activity relationship (SAR) of TPGS analogs, specifically on TPGS analogs where the PEG chain length was varied (Collnot et al., 2006, 2007). Those SAR studies revealed that rhodamine 123 (Rho) permeation rate through Caco-2 cell monolayers was strongly influenced by polyethylene glycol chain length, with an optimum linear PEG molecular weight between 1000 (**1**) and 1500 (**2**) Da. Recently, we conducted detailed studies to determine the mechanism by which TPGS reduces P-gp-mediated efflux and enhances oral bioavailability of certain compounds (Collnot et al., 2007). From these studies, the prevalent mechanism appears to be ATPase inhibition. The data are not consistent with competitive inhibition or unspecific cell membrane rigidity/fluidization; rather, ATPase inhibition appears to occur from blocking substrate binding and/or via P-gp allosteric modulation.

With this mechanistic understanding in hand, we sought to expand our SAR studies. Our goal was to create new, more powerful, surface-active inhibitors. We elected to design these new inhibitors such that, like TPGS, they would be constructed from non-toxic components, and thus have the best chance to provide good safety profiles. Safe but more potent inhibitors may have significant value (*e.g.* enabling smaller dosage forms and/or increasing drug payload). Herein, we present novel TPGS analog synthesis, *in vitro* P-gp inhibitor potency testing using the Caco-2 permeability model, and initial *in vivo* PK proof of concept.

2. Methods and materials

2.1. Materials

Non-essential amino acids, streptomycin and penicillin, *N*-2-hydroxyethylpiperazine-*N*′-2-ethane sulfonic acid (HEPES), Dulbecco's modified Eagle medium (DMEM), rhodamine 123 (Rho), cyclosporine A (CsA), carboxymethyl cellulose (CMCe; microgranular, 25–60 μM), microcrystalline cellulose (MCC), vinorelbine ditartrate salt, domperidone, chlorpromazine hydrochloride, prazosin hydrochloride, dexamethasone, diltiazem hydrochloride, raloxifene hydrochloride, loperamide hydrochloride, propranolol hydrochloride, methanol, acetonitrile, dichloromethane, iso-propyl alcohol, ethanol, water, formic acid, ammonium acetate, sodium hydroxide, polyethylene glycol 1000 (PEG-1000), PEG-750-OMe (methyl ether), PEG-1100-OMe, PEG-1500, PEG-2000, PEG-400, polypropylene (PPG) 1000, PPG-1000-MBE (monobutyl ether), PEG-PPG-MBE-970, PEG-PPG-PEG-1100, PEG-monooleate-860, cholesterol succinate, cholic acid, deoxycholic acid, pyridine, DMAP (4-dimethylaminopyridine), 4-chromanol, succinic anhydride, toluene, and DCC (*N*,*N*′-dicyclohexylcarbodiimide) were purchased from Sigma–Aldrich Chemical Company (St. Louis, MO). Heat-inactivated fetal calf serum (FBS) and Hank's Buffered Saline Solution (HBSS) were purchased from GIBCO (Invitrogen Corp.; Carlsbad, CA). Saquinavir base (Lot # 25449) was purchased from Apin Chemicals Ltd. (Abingdon, Oxon, UK). Raloxifene 6-glucuronide (Lot # 19-WG-9-1) and raloxifene 4′-glucuronide (Lot # 18-WG-171-1) were purchased from Toronto Research Chemicals, Inc. (North York, Ontario Canada). Wistar-Hannover plasma (potassium EDTA) was obtained from Bioreclamation Inc. (Hicksville, NY).

2.2. Caco-2 cell culture and handling

Caco-2 cells, clone C2BBe1, were purchased from American Type Culture Collection (ATCC; Manassas, VA). Cells from passage 49–55 were used. Caco-2 cell monolayers were grown on polyethylene terephthalate (PET) membranes (Falcon™ HTS Multiwell, 1.0 μm pore size, 0.31 cm^2 growth area, and 6.5 mm diameter) for 21–23

Table 1
Mass spectrometer conditions for compounds monitored using electrospray ionization positive ion mode (ESI+).

Compound	Mass transition	GS1/2	DP	CE	CXP	R/LOD[a]
Astemizole	459.2–135.1 *m/z*	15/20	36.0	51.0	8.0	0.9966/0.03
Chlorpromazine	319.0–58.1 *m/z*	15/15	46.0	67.0	8.0	0.9959/0.02
Dexamethasone	393.2–373.2 *m/z*	20/10	36.0	13.0	12.0	0.9999/0.01
Diltiazem	414.9–178.1 *m/z*	15/10	51.0	35.0	6.0	0.9966/0.01
Domperidone	426.1–175.1 *m/z*	20/15	61.0	41.0	10.0	0.9975/0.01
Loperamide	477.2–266.2 *m/z*	10/10	61.0	37.0	6.0	0.9945/0.01
Propranolol	260.2–116.2 *m/z*	20/30	81.0	27.0	6.0	0.9974/0.01
Prazosin	384.3–95.0 *m/z*	15/15	56.0	71.0	16.0	0.9976/0.03
Raloxifene	474.3–111.7 *m/z*	15/15	80.0	45.0	8.0	0.9995/0.22[b]
Raloxifene Glucuronides	650.3–474.2 *m/z*	15/15	61.0	47.0	14.0	0.9996/0.10[b]
Rhodamine 123	345.2–285.2 *m/z*	20/20	91.0	61.0	16.0	0.9987/0.01
Saquinavir	671.3–570.3 *m/z*	10/10	61.0	47.0	14.0	0.9942/0.07
Vinorelbine	779.2–122.1 *m/z*	10/10	106.0	83.0	8.0	0.9963/0.08

[a] $1/x^2$ weighted (x = analyte concentration) linear regression standard curve ($N = 3 \pm$ S.D.) LOD = limit of detection (ng/mL); R = correlation coefficient, computed using the Pearson correlation with a two tailed P-value test ($P < 0.0001$) at a 95% confidence interval.
[b] LOD from plasma extracted samples.

days. Cells were seeded (density of ~60,000 cells/cm^2) and grown at 37 °C in a controlled atmosphere of 5% CO_2 with a relative humidity of 85%. The culture medium was changed every two days and consisted of DMEM supplemented with 10% FBS, 1% non-essential amino acids, 100 μg/mL streptomycin, and 100 U/mL penicillin. Transepithelial electrical resistance (TEER) was measured with an automated REMS electrical volt-ohm meter EVOM (World Precision Instruments; Sarasota, Florida). Monolayers with TEER values >350 Ω cm^2, with background subtracted, were used for transport studies.

2.3. Compound transport assay

Compound transport assays were performed in absorptive (apical to basolateral, Ap-to-Bl) and secretory (Bl-to-Ap) directions. To initiate the experiments, a solution of compound (10 μM) in buffer solution (37 °C)–HBSS containing 25 mM HEPES–(pH 6.5 for Ap-to-Bl; pH 7.4 for Bl-to-Ap) was added to the donor compartment and buffer solution (pH 6.5 for apical side, and pH 7.4 for basolateral side) was added to the receiver compartment. Samples were collected by complete receiver volume replacement with fresh buffer solution (37 °C) at 30, 60, 90, 120, 150, 180, 240, and 300 min. Compounds were quantified by LC/MS/MS.

2.4. Excipient screening assay

Rho (10 μM) transport was assessed in the secretory (Bl-to-Ap) direction in the presence of various surface-active agents (excipients, 30 μM); the excipient solutions were freshly prepared in HBSS/HEPES (37 °C). Prior to Rho transport experiments, the monolayers were pre-incubated for 1.0 h with the corresponding excipient on both sides at pH 7.4. Subsequently, at $t = 0$ min, a solution of Rho (10 μM, 1000 μL) in buffer/excipient solution (pH 7.4) was added to donor compartment (basolateral side) and pure buffer solution (pH 6.5) added to the receiver compartment (apical side, 300 μL). The method did not utilize plate-shaking. Samples were collected after 60, 120, and 180 min from the receiver compartment. Samples were collected by complete receiver volume replacement with fresh buffer solution (37 °C) containing excipient. Rho was quantified by LC/MS/MS.

2.5. Liquid chromatography mass spectrometry

We used an Applied Biosystems Sciex 4000-QTrap® (Applied Biosystems; Foster City, CA) equipped with a Shimadzu HPLC (Shimadzu Scientific Instruments, Inc.; Columbia, MD), a PEAK Scientific API Systems gas generator (PEAK Scientific; Bedford, MA) and Leap auto-sampler (LEAP Technologies; Carrboro, NC). Liquid chromatography employed an Agilent Technologies, Zorbax extended-C18 50 mm × 4.6 mm, 5 μm column at 40 °C with a flow rate of 0.4 mL/min. The mobile phase consisted of A: 10 mM ammonium acetate, 0.1% formic acid in water, and B: 50:50 acetonitrile:methanol. Two different HPLC methods were used. HPLC method 1 had a 6.5 min run time; started at 5% B, ramped up to 95% B at 3 min and held until 4.5 min, ramped back down to 5% B at 5 min and held until end of run. HPLC method 2 (for vinorelbine) had an 8.0 min run time; started at 20% B, ramped up to 70% B at 3 min and held until 3.9 min, ramped up to 95% B at 4.5 min and held until 6.5 min, ramped back down to 20% B at 7.0 min and held until end of run. In addition to the settings summarized in Table 1, the MS/MS conditions for the compounds monitored via electrospray ionization positive ion mode (ESI+) were: (i) an ion-spray voltage of 5500 V; (ii) temperature, 450 °C; (iii) nitrogen was used for the curtain gas (CUR) and collisionally activated dissociation (CAD) gas; (iv) CAD gas was set at medium; (v) ion source gas one (GS1) and two (GS2) were air; (vi) the entrance potential was set at 10.0 V; (vii) quadruple one (Q1) and three (Q3) were both set on unit resolution; (viii) dwell time was set at 200 ms; and (ix) declustering potential (DP), collision energy (CE), and collision cell exit potential (CXP) are voltages (V).

2.6. Apparent permeability and statistical analysis

Flux was determined using receiver compartment compound steady-state appearance rates ($\Delta Q/\Delta t$). P_{app} across Caco-2 monolayers was calculated via:

$$P_{app} = \frac{\Delta Q}{\Delta t A C_0}$$

P_{app} = apparent permeability coefficient [cm/s]; $\Delta Q/\Delta t$ = permeability rate [μg/s; pmol/s]; C_0 = initial concentration in donor chamber [μg/cm^3; pmol/cm^3]; and A = membrane surface area [cm^2]. P_{app} Ap-to-Bl, P_{app} Bl-to-Ap, and active transport are expressed as means ± standard deviation (S.D.). Efflux ratio (ER) was computed as:

$$ER = \frac{(P_{app}Bl \rightarrow Ap)}{(P_{app}Ap \rightarrow Bl)}.$$

Graphs were prepared using Prism 4.02™ (GraphPad Software, Inc.; San Diego, CA). Active transport K_m was computed from non-linear regression analysis.

2.7. Synthesis and purification

General synthetic procedure: vitamin E succinate (3.25 g, 6.12 mmol), or other starting carboxylic acid (*i.e.* chromanol succinate, steroid, bile salt), was dissolved in dichloromethane (20 mL) and 1.1 equivalents of the corresponding polyethylene glycol or polypropylene glycol added and stirred at room temperature. DMAP (0.1 equivalents) – in the case of the steroids, pyridine was used as the base – and DCC (1.1 equivalents) were then added. The reaction vessel was capped and stirred overnight. The reaction mixture was filtered through a Büchner funnel, and the filtrate concentrated under reduced pressure to afford crude product(s).

Reaction products (**1**–**16**) were purified (Fig. 1) via preparative HPLC (Varian Dynamax Microsorb C8 column, 250 mm × 41.4 mm i.d., 8 μm particles, 60 Å pore) using mobile phases: A, 70/30 [50/50 iso-propyl alcohol (IPA)/acetonitrile (ACN)]/0.0025 M NH_4OAc; B, 50/50 IPA/ACN; and C, 100% IPA with general step-gradient conditions of A for 24 min, B for 6 min and C for 12 min at a flow rate of 65 mL/min.

2.8. Mass spectrometric analysis of reaction mixtures and purified materials

Synthesized samples were analyzed by positive and negative ion LC–MS/MS on a Waters LCT time of flight mass spectrometer. The system was equipped with a Hewlett Packard Series 1100 on-line degasser, auto-sampler (2.0 mL vials), quaternary pump, column heater, and diode array UV–vis spectrometer. In order to enhance ionization, a solution of 25.0 mM ammonium acetate in methanol was added after the diode array at 0.10 mL/min using a Waters 510 pump. Approximately 130 μL of the total flow of 1.1 mL/min was split to the mass spectrometer and the remainder sent to waste. The separations were performed with a Varian HPLC column (150 mm × 4.6 mm, Microsorb 100-5 C8). Solvent A was a mixture of water (1000 mL containing 2.50 mM ammonium acetate) and 30.0 mL of organic (mixture of 50/50 (v/v) isopropanol/acetonitrile). Solvent B was a mixture of 50/50 isopropanol/acetonitrile. The following HPLC conditions were employed: a 38.0 min run time which started at 40% B was ramped to 100% B over 30.0 min, ramped to 60% B at 31.0 min and held until end of run. To obtain molecular weight information, various TOF mass spectrometry conditions were used: Cycle time (1.0 s), scan duration (0.5 s), inter-scan delay (0.5 s), retention window (0–30 min), mass ranges of 50–3000, capillary voltage of 2500 (ES−) and 3200 (ES+), RF lens voltage (100), desolvation temp 250 °C, source temp 90 °C, sample cone voltage (25 or 75), and diode array wavelength range of 190–900 nm. PPG and PEG components yielded $(M + NH_4)^+$ or $(M + 2NH_4)^{2+}$ ions in the positive ion mode and $(M + \text{acetate})^-$ ions in the negative ion mode. Many nitrogen containing by-products yielded $(M + H)^+$ ions in the positive ion mode and $(M - H)^-$ ions in the negative ion mode. All components produced the expected average molecular weight values.

2.9. Raloxifene formulations and pharmacokinetic study design

2.9.1. Wister-Hannover rat study

In vivo testing was conducted at RCC Ltd. (Toxicology, CH-4452 Itingen, Switzerland). Male Wistar-Hannover rats (weight range, 257–313 g) were obtained from RCC Ltd. (Laboratory Animal Services, CH-4414 Füllinsdorf, Switzerland). Prior to dosing, rats were individually housed in Makrolon type-3 cages with wire mesh tops and standardized softwood bedding (Lignocel Schill AG, CH-4132 Muttenz/Switzerland). The room was air-conditioned with 10–15 air changes per hour, and maintained at 22 ± 4 °C and a relative humidity between 30 and 70%. The rats were subjected to 12 h fluorescent light/12 h dark cycles with music during the light period. The animals were allowed free movement and access to water.

The study design and metabolite investigations have been previously described in detail (Wempe et al., 2007a). Briefly, groups of four male Wistar-Hannover rats (300–350 g) were used. Group 1 received an HBenBCD/raloxifene solution (equivalent to 3.66 mg raloxifene base/mL); HBenBCD was present to ensure a raloxifene solution and not a suspension for the iv dose. Group 2 received capsules containing raloxifene dispersed in microcrystalline cellulose (MCC) (399 mg raloxifene/g). Group 3 received a raloxifene/propylene glycol oral solution containing 99.9 mg/g of raloxifene. Group 4 received a solution prepared by dissolving TPPG 1000 (**12**, 30 mg) in raloxifene/PG solution (same solution used for Group 3; 601 mg).

Group 1 (iv; 2.5 mg/kg) was dosed using a 1.0 mL syringe at an infusion rate of 0.30 mL per min. Oral dosage forms comprised capsules (solid and liquid filled) containing raloxifene formulation (Group 2, raloxifene/MCC, 10 mg/kg; Group 3, raloxifene liquid-filled capsules, 10 mg/kg; Group 4, raloxifene liquid-filled capsules 10 mg/kg with (**12**), 5.0 mg/kg) in gelatin Torpac Lock ring gel size 9 capsules (Torpac, USA). Using the Torpac dosing syringe (Torpac, USA), Groups 2–4 were dosed by capsule oral gavage followed by water (0.50 mL) to facilitate movement to the stomach. Animals were allowed free access to food and water, but were fasted for at least 8 h prior to dosing until 5 h post-dose. Dosing was 2–3.5 h after the beginning of a light cycle and dosing time across each group was consistent to avoid confounding chronopharmacokinetic effects.

Blood samples (300 μL) were collected from a catheter inserted into the jugular vein using an AccuSampler® (DiLab®; Oresund, Sweden). For Group 1 (iv), blood samples were taken at 0.083 (5 min), 0.25 (15 min), 0.50 (30 min), 1.0, 2.0, 3.0, 4.0, 5.0, 6.0, 8.0, 12.0, 24.0, 36.0, 48.0, and 72.0 h. Groups 2–4 were taken at 0.33 (20 min), 0.50 (30 min), 0.75 (45 min), 1.0, 2.0, 3.0, 4.0, 5.0, 6.0, 8.0, 12.0, 24.0, 36.0, 48.0, and 72.0 h. After each blood draw, removed blood volume was replaced by an equivalent volume of intraperitoneal saline. Blood samples were centrifuged at RCC Ltd. and plasma transferred into a designated well of a 96-well plate. The plates were stored on dry ice during filling and shipped frozen on dry ice. All animals were euthanized 72 h post-dose following terminal blood collection via abdominal aorta or cardiac puncture. Animals were anesthetized by CO_2/O_2 for collection followed by exsanguination.

An internal standard (IS) solution was freshly prepared in a 500 mL volumetric flask containing 1:1 (v/v) acetonitrile:methanol and saquinavir base (0.04 μM). Individually, the 96-well plates were removed from the freezer (−80 ± 10 °C) and allowed to warm to ambient temperature (45–50 min). The *in vivo* plasma samples (50 μL) were transferred into separate 1.5 mL micro-centrifuge tubes. Total plasma volume was brought to 100 μL by adding (50 μL) male Wistar-Hannover plasma (potassium EDTA). Subsequently, 200 μL of IS solution was added, capped, mixed (5 s), and centrifuged at 13,200 rpm (10.0 min) using an Eppendorf minispin centrifuge (Hamburg, Germany). The supernatant (250 μL) was transferred into individual wells of a 96-well plate. The 96-well plate was sealed and centrifuged at 3000 rpm (10.0 min) at 10 °C (Labofuge 400R Centrifuge). The 96-well plate was placed into the auto-sampler cool-stack (6 °C) and analyzed by a previously described validated LC/MS/MS method (Wempe et al., 2007a).

2.9.2. Sprague-Dawley rat study

This in-life study was conducted at East Tennessee State University – Quillen College of Medicine, Division of Laboratory Animal Resources (Johnson City, Tennessee, USA). The animal facility is AAALAC accredited. All procedures were reviewed and approved by the ETSU Committee on Animal Care. Male rats were purchased from Harlan World Headquarters (Indianapolis, Indiana, USA). Animals were housed in groups of three at 72 ± 2 °F and 55 ± 15%

humidity. Animals were allowed free movement and access to water with 12 h dark and light cycles. Dosing occurred ~2.0–2.5 h after the beginning of a light cycle. All animals had access to water, *ad libitum*, and were fasted for 14–16 h prior to dosing; food was returned 4 h post-dose.

Using tail-vein collection (*i.e.* the anterior portion of the tail ~2–3 mm was transected), blood samples (~125 μL) were collected (1.0, 1.5, 2.0, 2.5, 3.0, 3.5, 4.0, 4.5, 5.0, 6.0, 8.0 and 24 h post-dose) using mini-capillary blood collection tubes (~125 μL) that contained EDTA di-potassium salt (SAFE-T-FILL®; RAM Scientific Inc., Yonkers, NY, USA). Immediately after filling individual samples, the tubes were mixed and stored on dry ice and kept frozen (−80 ± 10 °C) until sample preparation and subsequent LC/MS–MS analysis. Control blood was collected from fasted, non-dosed, animals ($n = 3$) via inferior vena cava bleeding. In an analogous procedure as previously described, a raloxifene standard curve from extracted blood was prepared.

Raloxifene/CMCe and raloxifene/surfactant/CMCe formulations were prepared as follows: CMCe (2.0 g) was weighed out into a glass vial. Next, the non-ionic surfactant – TPGS 1000, Cholic PEG1000, or TPPG 1000 (all a purity of ≥99%) – was added (1.0 g). Ethanol (2.0 mL) was then added and homogenized (3–4 min) using a Polytron® PT1200 (Kinematica, CH; PT-DA 1212/2 EC). Afterwards, the homogenizer tip was washed in multiple portions with additional solvent (aqueous ethanol; 1–2 mL) and the combined contents were frozen (*i.e.* liquid nitrogen) and lyophilized (36–38 h). Next, in a ratio of 1:3 (raloxifene hydrochloride:CMCe/Surfactant; w/w), formulations were prepared by mixing via a mechanical roller (1 h). Thereafter, to help remove clumps or aggregates that might have formed the material was removed and passed through a 35-mesh screen. After additional mixing (45 min), using the Torpac filling funnel, the formulations were filled into hard shell Torpac Lock Ring Gel Capsules (Size 9, *in vivo* dosing). Therefore, these PK capsules contained a surfactant:raloxifene HCl ratio of ~1:1 (w/w). Using the Torpac dosing syringe (Torpac, USA), capsule oral gavage dosing was conducted; water (0.50 mL) was immediately orally dosed to facilitate capsule movement to the stomach.

2.9.3. Raloxifene formulation solubility comparison

As an attempt to rank order the *in vitro* solubility enhancement of raloxifene by **1**, **15** and **12**, the following was performed: to mimic the initial *in vivo* dose conditions, formulation amounts equal to the *in vivo* dose were weighed out (in triplicates) into separate glass vials. Water (HPLC grade, 500 μL) was added and the contents mixed at room temperature (400 rpm; 10 min) and immediately filtered through a 0.45 μm filter (Acrodisc® Premium Ion Chrom Syringe Filter; Pall Life Sciences, Ann Arbor, MI); the filtrates were analyzed by LC/MS–MS.

2.10. CMC determination

Critical micelle concentrations, CMC, for **1**, **12**, and **15** were obtained from the concentration dependence of the surface tensions of their solutions in water at ambient temperature. Solutions of each material were obtained by serial dilution of an initial solution prepared by weight. The surface tension of each solution was determined from the force exerted by the meniscus on a glass cover-slip as it was slowly immersed and retracted from the liquid in a Cahn DCA-322 Dynamic Contact Angle Analyzer (Cahn Instruments, Madison, WI). A fresh cover-slip, passed through the oxidizing region of a gas flame at least three times on each side, was used for each measurement. The CMC was taken to be the break point, above which the surface tension ceased to decrease with increasing concentration.

2.11. Statistical methods

Statistical analysis on the effects of *in vitro* permeability, pH comparisons, efflux ratio (ER), and excipient comparisons were performed either using an unpaired *t*-test with Welch's correlation or a one way-ANOVA with Dunnett's multiple comparison post-test at the 95% confidence level. The effect of TPGS 1000 purity on *in vitro* IC_{50} was assessed using an unpaired *t*-test. The formulation groups, for the Wistar-Hannover experiments, were compared with respect to 'Area Under the Curve' (AUC), T_{max}, C_{max}, total exposure, and absolute bioavailability (F) using a one-way ANOVA followed by a Dunnett's multiple comparison test ($P < 0.05$ denotes significance). The Sprague-Dawley rat data were compared via repeated measures tests with a Friedman (nonparametric) test followed by a Dunn's post test at the 95% confidence level.

3. Results and discussion

3.1. Inhibitor design and synthesis

Fundamentally, TPGS contains a hydrophile (PEG) attached through a linker (succinic acid) to a hydrophobe (α-tocopherol) (Fig. 1). Previous studies investigated the relationship between PEG chain length and potency of Rho efflux inhibition (Collnot et al., 2006). These studies predicted optimal P-gp inhibition at a PEG chain length of approximately 24–33 monomer units. Subsequently, as part of an investigation of the TPGS efflux inhibition mechanism, we briefly examined the impact of varying the hydrophobe. We found that hydrophobic moieties such as cholesterol and phytol, replacing α-tocopherol in the basic TPGS structure, gave more potent P-gp inhibition than TPGS 1000 (Wempe et al., 2007b). Encouraged by these results, we decided to broaden our structure–property scope; we were searching for more potent inhibitors and hoped to gain further SAR insight. In the work reported herein, we elected to examine: (i) modified hydrophiles and their effects; and (ii) a broader range of hydrophobes. Design criteria included minimization of *in vivo* hydrolysis, and use of benign components. The structures are illustrated in Fig. 1 and Table 2. We investigated polyethylene glycol hydrophile replacement with polypropylene glycol (*e.g.* compound **12**) or with PEG and PPG copolymers (*e.g.* compound **10**). We compared hydrophobe α-tocopherol replacement with chromanol (compound **4**), cholic acid (compound **15**), 7-deoxycholic acid (compound **16**) and cholesterol (compound **14**). Since cholic acid and 7-deoxycholic acid possess carboxyl functionality, a linker for these hydrophobes to the hydrophile was not required. Inhibitor candidates were readily constructed by forming an ester linkage between an activated carboxylic acid and the hydrophile alcohol. The well known carbodiimide coupling reagent DCC in the presence of base (DMAP) was used, except with steroid hydrophobes where pyridine was used as the base (Smith and March, 2007).

3.2. Caco-2 cell monolayer validation

Confluent Caco-2 monolayers exhibit morphological and functional similarities to small intestinal epithelium. They possess metabolizing enzymes (*e.g.* glucuronidation, sulfation, esterase, etc.) and influx/efflux transporter proteins (*e.g.* glucose transporters and P-gp, respectively). Caco-2 monolayer experiments are known to produce *in vitro* permeability data that may correlate to human absorption (Rubas et al., 1993; Lennernäs, 1998; Cogburn et al., 1991; Yu et al., 1996). However, as with all *in vitro* techniques, experiments with Caco-2 monolayers have limitations; for example, they are known to possess little to no cytochrome P450 (called CYP or P450) activity (*i.e.* CYP3A4) and culture conditions are important

Table 2
Compound substituents summary.

Compound	Descriptor	Hydrophobe (R)	Linker	Glycol (G_{DP})	R′
1	TPGS 1000	α-Tocopherol	Yes	PEG_{22}	H
2	TPGS 1500	α-Tocopherol	Yes	PEG_{34}	CH_3
3	Chrom 400	Chromanol	Yes	PEG_{12}	H
4	Chrom 1000	Chromanol	Yes	PEG_{22}	H
5	TPGS 400	α-Tocopherol	Yes	PEG_{12}	H
6	TPGS 750-OMe	α-Tocopherol	Yes	PEG_{16}	CH_3
7	TPGS 1100-OMe	α-Tocopherol	Yes	PEG_{24}	CH_3
8	TPGS 2000	α-Tocopherol	Yes	PEG_{45}	H
9	TPGS 860-Oleate	α-Tocopherol	Yes	PEG_{13}	Oleate
10	TPGS PEG-PPG-PEG 1100	α-Tocopherol	Yes	PEG_1-PPG_{17}-PEG_1	H
11	TPGS PPG-PEG-OBu 970	α-Tocopherol	Yes	PPG_7-PEG_{11}	$(CH_2)_3CH_3$
12	TPPG 1000	α-Tocopherol	Yes	PPG_{16}	H
13	TPPG 1000-OBu	α-Tocopherol	Yes	PPG_{15}	$(CH_2)_3CH_3$
14	Chol 1000	Cholesterol	No	PEG_{22}	H
15	Cholic 1000	Cholic acid	No	PEG_{22}	H
16	Deoxycholic 1000	Deoxycholic acid	No	PEG_{22}	H

(Anderle et al., 1998; Carrière et al., 1994; Fisher et al., 1999). Furthermore, *in vitro* permeability may be influenced by a variety of experimental conditions such as passage number, membrane support type, plate-shaking, etc. (Takanaga et al., 1994; Nicklin et al., 1992; Karlsson and Artursson, 1991). Consequently, laboratories use permeability standards (*e.g.* mannitol and propranolol) to provide low and high apparent permeability (P_{app}) controls (Ogihara et al., 1999; Lu et al., 1996; Pade and Stavchansky, 1998).

Prior to evaluating the synthesized excipients, it was imperative to demonstrate that the *in vitro* Caco-2 system we were using was functioning appropriately. In addition to using a different membrane support, our previous *in vitro* studies did not incorporate a pH gradient (Collnot et al., 2006). The current studies incorporate a more physiologically relevant *in vitro* model, one with a pH gradient in the Ap-to-Bl (pH 6.5–7.4) direction. As summarized in Table 3, various compounds extending over a low to high *in vitro* permeability range were tested (10 μM). Loperamide had the highest efflux ratio (ER) (25.8 ± 6.0) and largest Bl-to-Ap P_{app} (754.0 ± 130.0 × 10^{-6} cm/s). For other compounds, ER's ranged between 13.7 ± 1.8 and 2.1 ± 0.2 for prazosin and dexamethasone, respectively. Rho and saquinavir ER's were between seven and nine and consistent with what others have reported (Rege et al., 2002; Alsenz and Haenel, 2003). The paracellular transport marker mannitol and the passive diffusion marker propranolol afford the expected ER of approximately one. Using CsA as a P-gp inhibitor, we observed the expected increase and decrease on Rho transport in both the Ap-to-Bl (9.1 ± 1.3 × 10^{-6} cm/s to 50.0 ± 4.2 × 10^{-6} cm/s) and Bl-to-Ap (117.0 ± 12.0 × 10^{-6} cm/s to 37.8 ± 3.4 × 10^{-6} cm/s) directions, respectively. Hence, CsA significantly altered Rho *in vitro* ER (0.8 ± 0.1). These results are important because they illustrate that the Caco-2 *in vitro* system contains P-gp and can be inhibited; in addition, a system where one may delineate materials over a wide permeability range.

Furthermore, many parameters may influence the interactions between P-gp and a substrate and/or inhibitor. These include overall enterocyte lipid content, bilayer physical state, aqueous buffer composition, whether the substrate and/or inhibitor operates by a classical 'lock-and-key' competitive inhibition, or some sort of surface-active modification that alters surface tension, surface potential, or perhaps a local dielectric constant. A Caco-2 monolayer Rho concentration dependent transport study without an inhibitor was conducted and the Ap-to-Bl and Bl-to-Ap steady-state (60–120 min) results are summarized in Fig. 2. Under the pH gradient conditions, efflux was saturated at a lower concentration; we observed a K_m of 24.7 ± 2.9 μM and 15.0 ± 2.2 μM for apical pH 7.4 and 6.5, respectively. For all concentrations, Rho transport rate (P_{app}) in the Ap-to-Bl direction was significantly ($P < 0.05$) lower under proton gradient conditions. On the other hand, the Bl-to-Ap differences did not become significant until Rho was ≥ 5 μM. Furthermore, altering apical pH 7.4–6.5 (10 μM Rho) changed the computed ER (10.5 ± 1.3–13.0 ± 1.5) and also illustrates the significant ($P < 0.0015$; unpaired *t*-test with Welch's correlation) influence of a proton gradient. The computed ER's at varying

Table 3
Absorptive transport (Ap-to-Bl), secretory transport (Bl-to-Ap), and efflux ratio (ER) across Caco-2 monolayers for various compounds (10 μM) with proton gradient; mean ± S.D., $n = 4$.

Compound (10 μM)	Ap-to-Bl (P_{app} ± S.D.)[c]	Bl-to-Ap (P_{app} ± S.D.)[c]	Efflux ratio (±S.D.)
Mannitol[b]	0.24 ± 0.07	0.23 ± 0.07	1.0 ± 0.4
Vinorelbine	1.1 ± 0.2	12.3 ± 1.0	11.8 ± 1.9
Domperidone	1.3 ± 0.1	9.7 ± 0.4	7.6 ± 0.5
Saquinavir	1.4 ± 0.2	11.3 ± 0.7	8.5 ± 1.0
Chlorpromazine	1.5 ± 0.1	17.3 ± 2.8	11.7 ± 1.8
Prazosin	5.1 ± 0.8	66.3 ± 4.6	13.7 ± 1.8
Rhodamine	9.1 ± 1.3	117.0 ± 12.0	13.5 ± 1.9
Rhodamine + CSA (30 μM)[a]	50.0 ± 4.2 ***	37.8 ± 3.4 ***	0.8 ± 0.1 ***
Dexamethasone	21.2 ± 1.1	43.2 ± 3.6	2.1 ± 0.2
Diltiazem	22.4 ± 0.7	117.0 ± 6.0	5.3 ± 0.3
Loperamide	29.9 ± 5.8	754.0 ± 130.0	27.0 ± 6.0
Propranolol	124.0 ± 25.0	111.0 ± 22.0	1.0 ± 0.2

[a] Rho vs Rho + CsA, unpaired *t*-test with Welch's correlation.
[b] Values obtained with [^{14}C]Mannitol at 5 μM (Wempe, 2003).
[c] $P_{app} \times 10^{-6}$ cm/s.
*** *P*-value <0.001.

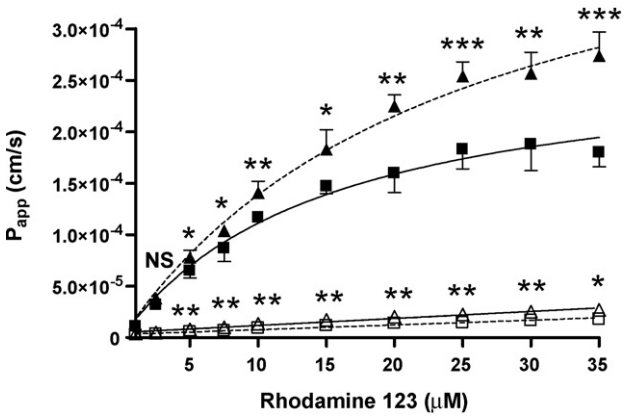

Fig. 2. Rho Caco-2 monolayer concentration dependent transport (absorptive transport, Ap-to-Bl; secretory transport, Bl-to-Ap). (△) Ap-to-Bl, Ap pH 7.4; (▲) Bl-to-Ap, Ap pH 7.4; (□) Ap-to-Bl, Ap pH 6.5; (■) Bl-to-Ap, Ap pH 6.5; mean ± S.D., $n = 4$.

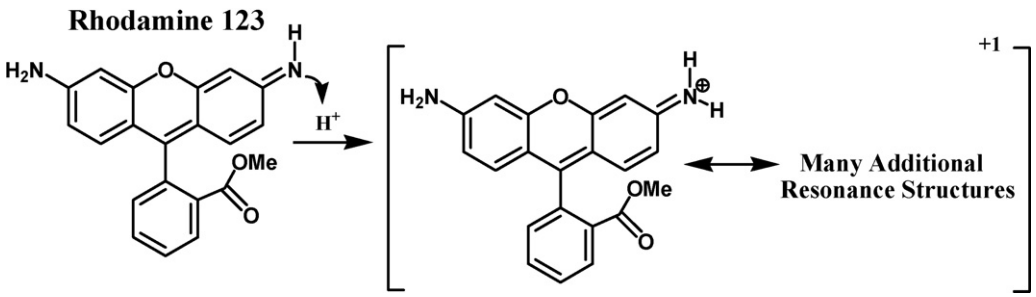

Fig. 3. Rhodamine 123.

concentrations of Rho were statistically significant between 5 and 15 μM.

As depicted in Fig. 3, under acidic conditions, a basic compound like Rho may exist in two forms, neutral and protonated; pronotated form generates an extremely resonance stabilized positively charged material. Changing to an acidic pH gradient (*e.g.* apical pH 7.4 to 6.5) presumably pushes this equilibrium to the right, LeChâtelier's principle. The extensive delocalization of Rho-H^+ causes it to cross the membrane more slowly, as in the case of verapamil where protonation impedes trans-membrane movement (Cullis et al., 1997; Ferté, 2000). A known P-gp substrate, Rho has a lower cellular accumulation in P-gp expressing cells than in P-gp deficient cells (Ferté, 2000). At 10 μM, Rho appears to be transported through both –H and –R P-gp binding sites (Shapiro and Ling, 1998). Consequently, we selected Rho (10 μM) as our excipient screening assay.

3.3. Excipient in vitro screening

The *in vitro* screening results, for the novel inhibitors in a Caco-2 monolayer model with Rho as the substrate, are summarized in Fig. 4. We included TPGS 1000 and cyclosporine A (CsA) as positive controls, Rho alone as a negative control, and PEG 1000 and PPG 1000 for comparative purposes. As previously observed (Collnot et al., 2007), TPGS analogs having higher and lower molecular weight

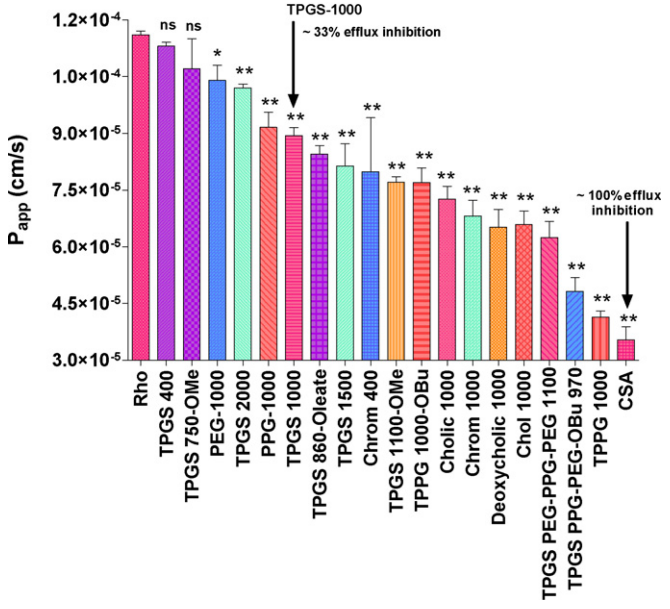

Fig. 4. Caco-2 cell monolayer Bl-to-Ap steady-state (60–120 min) inhibition of Rho (10 μM) in the presence of excipient (30 μM); mean ± S.D., $n = 4$. Groups were compared to Rho. One-way ANOVA followed by a Dunn's multiple comparison test: ns = not significant; **P*-value <0.05; ***P*-value <0.01.

PEG tails (**5**, **6**, **8**) were weak inhibitors, as were PEG 1000 and PPG 1000. TPGS 1000 (**1**; 30 μM) reduced Rho *in vitro* efflux by 33 ± 2% and CsA afforded complete *in vitro* efflux inhibition. TPGS PEG side chain modification, by capping with an oleate ester group (**9**), gave slight efflux inhibition enhancement vs. **1**; furthermore, TPGS with a PEG tail of molecular weight 1500 (**2**) came close to the predicted optimum.

Hydrophobe modification began to show more profound effects. Replacement of α-tocopherol with chromanol created a significantly more potent inhibitor (**4**, 59 ± 3% efflux inhibition). As with TPGS, reduction in the molecular weight of the PEG side chain in the chromanol analog afforded a weaker inhibitor (**3**, 45 ± 15% efflux inhibition), but the difference between the two was not statistically significant. As observed previously (Collnot et al., 2007), replacement of α-tocopherol with cholesterol gave a more potent inhibitor (**14**, 62 ± 1% efflux inhibition). Furthermore, the cholic acid (**15**, 54 ± 1% efflux inhibition) and deoxycholic acid (**16**, 63 ± 3% efflux inhibition) analogs, having no succinate linker, were significantly more potent than TPGS 1000 (**1**).

We obtained even more interesting results when the nature of the hydrophile was modified, leaving α-tocopherol as the hydrophobe. Changing a PEG side chain to a PEG-PPG copolymer of similar chain length (**10**), we obtained an inhibitor (66 ± 3% efflux inhibition) that was slightly more potent than the cholesterol analog. Capping a PEG-PPG copolymer side chain with *n*-butyl ether (**11**, 85 ± 1% efflux inhibition) afforded an even more potent inhibitor. However, the most potent inhibitor of the entire series was obtained with a pure PPG side chain having a molecular weight equivalent to that of the PEG side chain of TPGS 1000. This new analog, TPPG 1000 (**12**), afforded 93 ± 2% Rho efflux inhibition in this *in vitro* Caco-2 monolayer model. The potency of **12** closely approached that of CSA in this assay and was a highly encouraging result with respect to dosage size reduction and/or active payload increase potential.

In summary, these *in vitro* results help to illustrate well known phenomena regarding non-ionic surfactants; physiochemical properties (*i.e.* hydrophobic/hydrophilic modification) are very important. An excellent review on this topic was described in 1998 by Uchegbu and Vyas; therefore we do not provide an overview in this report. None the less, two major aspects of the non-ionic surfactant include: (1) its inherent ability to form niosomes (Uchegbu and Vyas, 1998); and (2) the attributes required to cause P-gp inhibition. In these Caco-2 studies, we used non-ionic surfactants at a concentration of 30 μM; a TPGS 1000 concentration of 30 μM (<0.005 wt%) was well below the reported CMC (0.02 wt%) of TPGS 1000 and other related analogs (Collnot et al., 2006, 2007) in Caco-2 buffer solution. These experimental conditions and results suggest that micelle formation was not prevalent in the Caco-2 experiments and that both the hydrophobic and hydrophilic ends on the non-ionic surfactant be important attributes to induce P-gp modulation. These statements are further supported by the fact that TPGS 400 is a better *in vitro* and *in vivo* drug solubilizer than TPGS 1000 (tamoxifen, not a P-gp substrate, PK data not shown), yet TPGS 400 afforded no

statistically significant difference in Rho 123 *in vitro* efflux compared to control. Therefore, a hydrophilic PEG, PPG, or combined PEG/PPG length between 900 and 1600 Da appears to be optimal to modulate drug efflux and the optimal length a function of the hydrophobe moiety.

3.4. In vivo oral absorption

We chose to examine briefly, and in preliminary fashion, the *in vivo* performance of our most promising inhibitor candidate, TPPG 1000 (**12**). We wanted to test its ability to enhance oral bioavailability of a drug with the following characteristics: P-gp substrate, poor oral bioavailability, and poor solubility. The osteoporosis drug raloxifene seemed to fit all of our criteria, so we chose to examine the impact of **12** on raloxifene oral bioavailability in the rat. We compared raloxifene alone in oral and i.v. dosage forms, versus orally administered raloxifene in propylene glycol solution with and without added TPPG 1000; the dosage groups and protocols are described in the Experimental section.

In Fig. 5 we present profiles of raloxifene and raloxifene glucuronide plasma concentration versus time after administration of oral raloxifene or raloxifene/(**12**) formulation. For clarity, only the AUC_{0-12} data are shown. The PK data has been summarized in Table 4. When administered orally in the absence of an inhibitor, raloxifene had very poor bioavailability (F). Upon dosing to male Wistar-Hannover rats, raloxifene powder filled capsules had $F = 2.6 \pm 0.4\%$; dosing liquid-filled capsules of raloxifene in propylene glycol (PG) did not substantially improve matters ($F = 2.7 \pm 0.6\%$). In contrast, orally administered liquid-filled capsules of raloxifene/PG solution containing TPPG 1000 roughly doubled the raloxifene bioavailability (Group 4, $F = 5.1 \pm 0.8\%$).

Raloxifene is rapidly and substantially metabolized in the gut, largely to glucuronides (Kemp et al., 2002). In the case of oral raloxifene capsule dosing (Group 2), T_{max} occurred at 4 h for both drug and glucuronides. In accord with the literature, Phase II drug metabolism was far more significant ($P < 0.0001$) via oral administration than by the intravenous route (ratio of raloxifene glucuronides AUC/raloxifene AUC = 0.52 ± 0.20 (oral) vs. 0.062 ± 0.012 (IV)). Also, after dosing with raloxifene/PG and raloxifene/PG (**12**) liquid-filled capsules, raloxifene phase II metabolism (Groups 3 and 4) was statistically ($P < 0.01$) more extensive (raloxifene glucuronides AUC/raloxifene AUC = 1.28 ± 0.60 and 1.21 ± 0.49, respectively) than control (Group 2). While raloxifene T_{max} values were fairly constant across all other groups, Group 4 (containing TPPG 1000) raloxifene glucuronide T_{max} values were considerably shorter and indicative of a more rapid raloxifene absorption and metabolism in the presence of inhibitor **12**. Furthermore, when the animals were administered raloxifene/PG (**12**) liquid-filled capsules (Group 4), the $AUC_{0-72\ h}$ values for raloxifene glucuronides were significantly ($P < 0.01$) larger than control (Group 2). Since raloxifene undergoes extensive pre-systemic metabolism, measurement of raloxifene levels alone may not provide the best indication of raloxifene uptake from the intestine into the portal blood. A better measure of the effect of **12** on total raloxifene absorption may be 'total raloxifene exposure', measured as (AUC raloxifene + AUC metabolites)/raloxifene dose. Using this combined measure (Table 4), it can be seen that administering raloxifene as raloxifene/PG/(**12**) liquid-filled capsules caused a 2.4-fold increase in total raloxifene exposure.

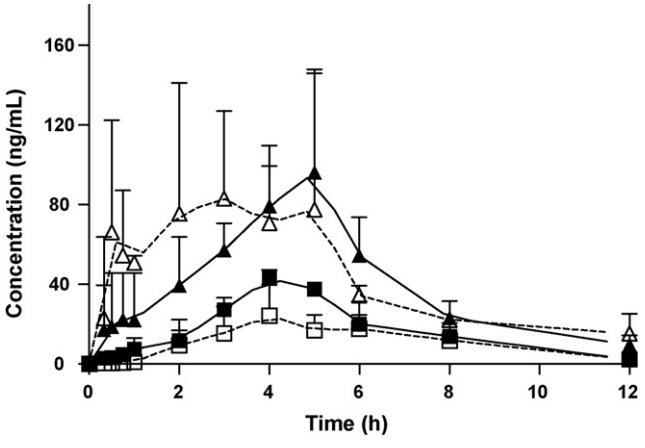

Fig. 5. Mean concentration (ng/mL; $n = 4 \pm$ S.D.) of raloxifene and raloxifene glucuronides from oral administration of solid raloxifene [(■) raloxifene; (□) raloxifene glucuronides] and raloxifene/PG/TPPG 1000 liquid-filled capsules [(▲) raloxifene; (△) raloxifene glucuronides].

These *in vivo* data provide initial evidence for BA enhancement of a poorly soluble P-gp substrate (*i.e.* raloxifene) in the presence of a novel non-ionic surfactant (*i.e.* TPPG 1000). However, one may argue that the observed *in vivo* enhancement was a function of improved drug solubility by TPPG 1000 in aqueous media after dosing and/or enhanced permeability by the PG400 present in the liquid-filled formulation. TPGS 1000 (**1**) and Cholic PEG1000 (**15**) are waxy solids at room temperature; whereas TPPG 1000 (**12**) is a thick liquid at room temperature. In water at ambient temperature ($24 \pm 1\ ^\circ C$), TPGS 1000 (**1**) exhibited a CMC ~0.01 g/100 mL with a limiting surface tension of 40 dyne/cm. TPPG 1000 (**12**) had a CMC of ~0.001 g/100 mL and a limiting surface tension of 39 dyne/cm. Cholic PEG1000 (**15**) does not appear to exhibit a CMC in water, but showed continuous decrease in surface tension up to 0.19 g/100 mL, the highest concentration tested. Furthermore, a recent communication describes that low surfactant concentrations may inhibit drug precipitation (Dai et al., 2008); therefore, the above-mentioned argument appears plausible. In our hands, raloxifene had an aqueous solubility of 0.33 ± 0.05 mg/mL at a pH of 4.0; lower raloxifene concentrations were observed in various buffers such as phosphate (pH 3.0, 6.5, and 7.3), and citrate (pH 3.2 and 4.8) (Wempe et al., 2007a). A 10 mg/kg dose, assuming a rat weight of 300 g, equates to 3.0 mg of raloxifene; a 500 μL bolus of water immediately after the capsule dose suggests that at best 5–6% of the raloxifene/MCC dose be in solution via the acidic GI condition. However, solubility testing in the presence of simulated gastric fluid was not performed in the past studies.

Consequently, additional *in vivo* experiments were performed (*i.e.* 20 mg/kg raloxifene in the presence of CMCe with or without 20 mg/kg non-ionic surfactant) using male Sprague-Dawley rats. For these additional *in vivo* studies, raloxifene/CMCe and raloxifene/surfactant/CMCe solid formulations were prepared; PG400 was avoided. As summarized in Fig. 6, TPGS 1000 (a known solubilizer and weak *in vitro* P-gp inhibitor) was found to enhance the BA; the control AUC_{0-24} was 115 ± 16 ng h/mL and statistically increased ($P < 0.05$) to 304 ± 17 ng h/mL in the presence of **1**. Hence, we attribute the majority of the observed increase in the presence of TPGS 1000 to be via *in vivo* solubilization enhancement. One may obtain aqueous TPGS 1000 solutions as high as 20 wt%. In addition, since **15** was prepared from a polyethylene glycol material, one might expect to observe similar solubilization enhancement via **15**. On the other hand, inherently derived from polypropylene glycol versus polyethylene glycol, TPPG 1000 (**12**) has poor water solubility compared to TPGS 1000 (**1**) and Cholic PEG1000 (**15**) (Bauduin et al., 2005). This translates to a much lower inherent potential to solubilize raloxifene; the formulation solubility experiments (see Section 2.9.3) afforded an intrinsic solubility trend of **1** > **15** > **12** > control. The AUC_{0-24} (Fig. 6) in the presence of **15** was 550 ± 162 ng h/mL, while in the presence of **12** it was 766 ± 109 ng h/mL; both were statistically increased ($P < 0.01$) rela-

Table 4
Raloxifene groups and pharmacokinetic parameter summary.

GRP	Formulation	Analyte	$AUC_{0-72\,h}$ (ng h/mL)	T_{max} (h)	C_{max} (ng/mL)	Total exposure[c]	F^{e} (%)
Intravenous							
1	Raloxifene solution	Raloxifene	11860 ± 1544[a]	< 5 min	2800 ± 432[a]	1424 ± 165	100
		Glucuronides[d]	728 ± 108[a]	0.25 ± 0.10	206 ± 43[a]		
Oral							
2	Raloxifene (capsules)	Raloxifene	300 ± 41	4.0 ± 0.5	42.9 ± 4.2	55 ± 10	2.6 ± 0.4
		Glucuronides[d]	153 ± 55	4.0 ± 0.5	24.3 ± 15.6		
3	Raloxifene/PG[b] (liq. fill capsules)	Raloxifene	321 ± 76 ns	5.0 ± 0.5 ns	46.5 ± 41.8 ns	94 ± 23 ns	2.7 ± 0.6 ns
		Glucuronides[d]	391 ± 152 ns	5.0 ± 0.5*	54.3 ± 40.9 ns		
4	Raloxifene/PG/TPPG 1000 (liq. fill capsules)	Raloxifene	602 ± 80**	4.5 ± 0.5 ns	87.8 ± 39.2 ns	132 ± 35**	5.1 ± 0.8**
		Glucuronides[d]	719 ± 271**	2.5 ± 0.5**	79.2 ± 51.9 ns		

Groups 3–4 were compared to Group 2. One-way ANOVA followed by a Dunn's multiple comparison test: ns = not significant.
* *P*-value <0.05.
** *P*-value <0.01.
[a] $=AUC_{0-72}$ are normalized to a 10 mg/kg dose.
[b] ($N = 3$).
[c] Total raloxifene exposure = [(AUC raloxifene + AUC glucuronide)/Raloxifene dose].
[d] Glucuronides are concentration of raloxifene 6-β-glucuronide + raloxifene 4'-β-glucuronide.
[e] Oral bioavailaility was calculated using the AUC_{0-72} for raloxifene only, not raloxifene + metabolites.

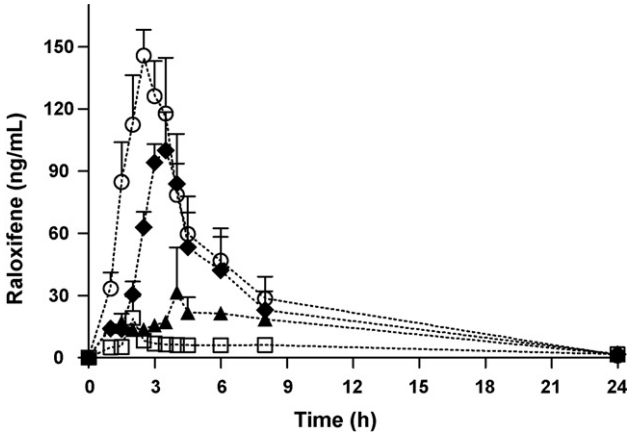

Fig. 6. Mean concentration (ng/mL; $n = 3 \pm$ S.D.) of raloxifene from oral administration of different formulations: raloxifene/CMC (□); raloxifene/TPGS 1000/CMC (▲); raloxifene/Cholic PEG1000/CMC (♦); and raloxifene-/TPPG 1000/CMC (○).

tive to control. These data further illustrate, relative to TPGS 1000 (**1**), that an enhancement in AUC of raloxifene was observed in the presence of **15** and **12**, presumably via enhanced efflux inhibition.

4. Conclusion

These studies were intended to identify promising P-gp inhibitor candidates from a family of non-ionic surfactants which are structurally related to the hydrophobe-linker-hydrophile construct present in TPGS 1000. Our expanded SAR studies have captured several promising new candidates. Using TPGS 1000 as the fundamental template, the hydrophobe α-tocopherol may be replaced by cholic acid, deoxycholic acid, cholesterol, or chromanol. These new inhibitors (**4**, **14**–**16**), relative to TPGS 1000, had superior *in vitro* performance. Hydrophile replacement proved even more beneficial, with PPG derivatives performing particularly well. The most promising P-gp inhibiting analog from this research was TPPG 1000 (**12**), where the TPGS 1000 PEG side chain was replaced with a PPG side chain of equal molecular weight. This analog not only approached the *in vitro* potency of a well-known P-gp inhibitor (CsA), but worked *in vivo* to afford a statistically significant enhancement in raloxifene (a P-gp substrate) bioavailability in rats. There is no reason, *a priori*, to believe that such TPGS 1000 modifications (*e.g.*, substitution of cholesterol for α-tocopherol, or substitution of PPG 1000 for PEG 1000) would substantially increase the toxicity of formulations containing these new inhibitors, though of course considerable safety testing will be required to confirm this belief.

These results are an important step towards rational inhibitor design; P-gp inhibitors designed to be (i) excipients; (ii) safe; and (iii) more potent P-gp inhibitors and enhancers of the bioavailability of orally administered drugs. They may, at a minimum, enable smaller dosage forms, and higher drug payloads in such dosage forms. Given the published literature on polymeric, non-ionic surfactant P-gp inhibitors, and the history of their identification and development, it was perhaps not predictable that one would be able to design members of this family that could compete with CsA in potency. These results are therefore highly promising toward safe and effective drug delivery systems development. Future work will encompass: (i) further expansion of the SAR work; (ii) safety testing of the most promising candidates; and (iii) *in vivo* bioavailability enhancement confirmation using additional P-gp substrate drugs, attempts to gain additional insight into the importance of drug/surfactant ratio, combinations of multiple non-ionic surfactants, *in vivo* food effects, etc.

References

Alsenz, J., Haenel, E., 2003. Development of a 7-day, 96-well Caco-2 permeability assay with high-throughput direct UV compound analysis. Pharm. Res. 20, 1961–1969.
Anderle, P., Niederer, E., Rubas, W., Hilgendorf, C., Spahn-Langguth, H., Wunderli-Allenspach, H., Merkle, H.P., Langguth, P., 1998. P-Glycoprotein (P-gp) mediated efflux in Caco-2 cell monolayers: the influence of culturing conditions and drug exposure on P-gp expression levels. J. Pharm. Sci. 87, 757–762.
Bauduin, P., Basse, A., Touraud, D., Kunz, W., 2005. Effect of short non-ionic amphiphiles derived from ethylene and propylene glycol alkyl ethers on the CMC of SDS. Colloids Surf. A: Physiochem. Eng. Aspects 270–271, 8–12.
Bogman, K., Erne-Brand, K.F., Alsenz, J., Drewe, J., 2003. The role of surfactants in the reversal of active transport mediated by multidrug resistance proteins. J. Pharm. Sci. 92, 1250–1261.
Brouwers, J., Tack, J., Lammert, F., Augustijns, P., 2006. Intraluminal drug and formulation behavior and integration in *in vitro* permeability estimation: a case study with amprenavir. J. Pharm. Sci. 95, 372–383.
Campbell, L., Abulrob, A.-N.G., Kandalaft, L.E., Plummer, S., Hollins, A.J., Gibbs, A., Gumbleton, M., 2003. Constitutive expression of P-glycoprotein in normal lung alveolar epithelium and functionality in primary alveolar epithelial cultures. J. Pharm. Exp. Ther. 304, 441–452.
Carrière, V., Lesuffleur, T., Barbat, A., Rousset, M., Dussaultz, E., Costet, P., Waziers, I., Beaune, P., Zweibaum, A., 1994. Expression of cytochrome *P*-450 3A in HT29-MTX cells and Caco-2 clone TC7. FEBS Let. 355, 247–250.
Choo, E.F., Leake, B., Wandel, C., Imamura, H., Wood, A.J.J., Wilkinson, G.R., Kim, R.B., 2000. Pharmacological inhibition of P-glycoprotein transport enhances the distribution of HIV-1 protease inhibitors into brain and testes. Drug Met. Disp. 28, 655–660.

Cogburn, J.N., Donovan, M.G., Schasteen, C.S., 1991. A model of human small intestinal absorptive cells. 1. Transport barrier. Pharm. Res. 8, 210–216.
Collnot, E.M., Baldes, C., Wempe, M.F., Hyatt, J., Navarro, L., Edgar, K.J., Schaefer, U.F., Lehr, C.M., 2006. Influence of vitamin E TPGS poly(ethylene glycol) chain length on apical efflux transporters in Caco-2 cell monolayers. J. Control Release 111, 35–40.
Collnot, E.M., Baldes, C., Wempe, M.F., Kappl, R., Hüttermann, J., Hyatt, J., Edgar, K.J., Schaefer, U.F., Lehr, C.M., 2007. Mechanism of inhibition of P-glycoprotein mediated efflux by vitamin E TPGS: influence on ATPase activity and membrane fluidity. Mol. Pharm. 4, 465–474.
Cullis, P.R., Hope, M.J., Bally, M.B., Madded, T.D., Mayer, L.D., Fenske, D.B., 1997. Influence of pH gradients on the trans-bilayer transport of drugs, lipids, peptides and metal ions into large unilamellar vesicles. Biochim. Biophys. Acta 1331, 187–211.
Dai, W.-G., Dong, L.C., Li, S., Deng, Z., 2008. Combination of pluronic/vitamin E TPGS as a potential inhibitor of drug precipitation. Int. J. Pharm. 355, 31–37.
Ferté, J., 2000. Analysis of the tangled relationships between P-glycoprotein-mediated multidrug resistance and lipid phase of the cell membrane. Eur. J. Biochem. 267, 277–294.
Fisher, J.M., Wrighton, S.A., Watkins, P.B., Schmiedlin-Ren, P., Calamia, J.C., Shen, D.D., Kunze, K.L., Thummel, T.E., 1999. First-pass midazolam metabolism catalyzed by 1α,25-dihydoxy vitamin D_3-modified Caco-2 cell monolayers. J. Pharm. Exp. Ther. 289, 1134–1142.
Fromm, M.F., 2004. Importance of P-glycoprotein at blood-tissue barriers. Trends Pharmacol. Sci. 25, 423–429.
Higgins, C.F., 1992. ABC transporters: from micro-organisms to man. Annu. Rev. Cell Biol. 8, 67–113.
Karlsson, J., Artursson, P., 1991. A method for the determination of cellular permeability coefficients and aqueous boundary layer thickness in monolayers of intestinal epithelial (Caco-2) cells grown in permeable filter chambers. Int. J. Pharm. 71, 55–64.
Kemp, D.C., Fan, P.W., Stevens, J.C., 2002. Characterization of raloxifene glucuronidation *in vitro*: contribution of intestinal metabolism to presystemic clearance. Drug Metab. Disp. 30, 694–700.
Lankas, G.R., Wise, L.D., Cartwright, M.E., Pippert, T., Umbenhauer, D.R., 1998. Placental P-glycoprotein deficiency enhances susceptibility to chemically induced birth defects in mice. Reprod. Tox. 12, 457–463.
Lennernäs, H., 1998. Human intestinal permeability. J. Pharm. Sci. 87, 403–410.
Lu, S., Gough, A.W., Bobrowski, W.F., Stewart, B.H., 1996. Transport properties are not altered across Caco-2 cells with heightened TEER despite underlying physiological and ultra-structural changes. J. Pharm. Sci. 85, 270–273.
Miller, D.W., Batrakova, E.V., Kabanov, A.V., 1999. Inhibition of multidrug resistance-associated protein (MRP) functional activity with pluronic block copolymers. Pharm. Res. 16, 396–401.
Mizuno, N., Niwa, T., Yotsumoto, Y., Sugiyama, Y., 2003. Impact of drug transporter studies on drug discovery and development. Pharmacol. Rev. 55, 425–461.
Nicklin, P., Irwin, B., Hassan, I., Williamson, I., Mackay, M., 1992. Permeable support type influence the transport of compounds across Caco-2 cells. Int. J. Pharm. 83, 197–209.
Ogihara, T., Tamai, I., Tsuji, A., 1999. Structural characterization of substrates for the anion exchange transporter in Caco-2 cells. J. Pharm. Sci. 88, 1217–1221.
Pade, V., Stavchansky, S., 1998. Link between drug absorption solubility and permeability measurements in Caco-2 cells. J. Pharm. Sci. 87, 1604–1607.
Rege, B.D., Kao, J.P.Y., Polli, J.E., 2002. Effects of nonionic surfactants on membrane transporters in Caco-2 cell monolayers. Eur. J. Pharm. Sci. 16, 237–246.
Roninson, I.B., 1987. Molecular mechanism of multidrug resistance in tumor cells. Clin. Physiol. Biochem. 5, 140–151.
Rubas, W., Jezyk, N., Grass, G.M., 1993. Comparison of the permeability characteristics of a human colonic epithelial (Caco-2) cell line to colon of rabbit, monkey, and dog intestine and human drug absorption. Pharm. Res. 10, 113–118.
Shapiro, A.B., Ling, V., 1998. Stoichiometry of coupling of rhodamine 123 transport to ATP hydrolysis by P-glycoprotein. Eur. J. Biochem. 254, 189–193.
Smith, M.B., March, J., 2007. March's Advanced Organic Chemistry: Reactions, Mechanisms, and Structure, sixth ed. John Wiley & Sons, Inc., Hoboken, New Jersey.
Suzuki, H., Sugiyama, Y., 2000. Role of metabolic enzymes and efflux transporters in the absorption of drugs from the small intestine. Eur. J. Pharm. Sci. 12, 3–12.
Takanaga, H., Tamai, I., Tsuji, A., 1994. pH-dependent and carrier-mediated transport of salicylic acid across Caco-2 cells. J. Pharm. Pharmacol. 46, 567–570.
Thiebaut, F., Tsuruo, T., Hamada, H., Gottesman, M.M., Pastan, I., Willingham, M.C., 1987. Cellular localization of the multidrug-resistance gene product P-glycoprotein in normal human tissues. PNAS 84, 7735–7738.
Uchegbu, I.F., Vyas, S.P., 1998. Non-ionic surfactant based vesicles (niosomes) in drug delivery. Int. J. Pharm. 172, 33–70.
Ueda, K., Cornwell, M.M., Gottesman, M.M., Pastan, I., Roninson, I.B., Ling, V., Riordan, J.R., 1986. The Mdrl gene, responsible for multidrug-resistance, codes for P-glycoprotein. Biochem. Biophys. Res. Comm. 141, 956–962.
Van der Valk, P., van Kalken, C.K., Ketelaars, H., Broxterman, H.J., Scheffer, G., Kuiper, C.M., Tsuruo, T., Lankelma, T.J., Meijer, C.J., Pinedo, H.M., 1990. Distribution of multi-drug resistance-associated P-glycoprotein in normal and neoplastic human tissues. Analysis with 3 monoclonal antibodies recognizing different epitopes of the P-glycoprotein molecule. Ann. Oncol. 1, 56–64.
Wempe, M.F., 2003. Intestinal epithelial cell (Caco-2) monolayers: sugar mechanistic studies. In: 45th Annual Land O'Lakes Conference, Devil's Head Resort, Merrimac, WI.
Wempe, M.F., Wacher, V.J., Ruble, K.M., Ramsey, M.G., Edgar, K.J., Buchanan, N.L., Buchanan, C.M., 2007a. Pharmacokinetics of raloxifene in male Wistar-Hannover rats: influence of complexation with hydroxybutenyl-beta-cyclodextrin. Int. J. Pharm. 346, 25–37.
Wempe, M.F., Hyatt, J., Zima, G., Edgar, K.J., 2007. Compounds Exhibiting Efflux Inhibitor Activity and Compositions and Uses Thereof. U.S. Provisional Patent Application No 60/788,053.
Yu, L.X., Lipka, E., Crison, J.R., Amidon, G.L., 1996. Transport approaches to the biopharmaceutical design of oral drug delivery systems: prediction of intestinal absorption. Adv. Drug Del. Rev. 19, 359–376.
Yu, L., Bridgers, A., Polli, J., Vickers, A., Long, S., Roy, A., Winnike, R., Coffin, M., 1999. Vitamin E-TPGS increases absorption flux of an HIV protease inhibitor by enhancing its solubility and permeability. Pharm. Res. 16, 1812–1817.